The mass transfer coefficient assessment and productivity enhancement of a vertical tubular solar brackish water still

HOU Jing[a,b], YANG Ju-Cai[a], CHANG Ze-Hui[c]*, ZHENG Hong-Fei[d], SU Yue-Hong[e]

([a] School of Chemical Engineering College, Inner Mongolia University of Technology, Hohhot 010051 China; [b] College of mechanical electrical heating and ventilation engine, Inner Mongolia Technical College of Construction, Hohhot 010070, China; [c] College of Energy and power engineering, Inner Mongolia University of Technology, Hohhot 010051, China; [d] School of Mechanical engineering, Beijing Institute of Technology, Beijing 100081, China; [e] Institute of Sustainable Energy Technology, Department of Architecture and Built Environment, University of Nottingham, Nottingham NG7 2RD, UK)

ABSTRACT: This paper presents an experimental investigation of a single-effect vertical tubular solar brackish water desalination device, with an aim to determine the mass transfer coefficient and its enhancement. The device consists of two closely spaced concentric pipes. The outside of the inner pipe is covered with a wicking material and wetted with hot brackish water. The water vapor evaporated from the wicking material condenses on the inside of the outer pipe. The measured productivity and temperatures at various points are given for different wicking materials thickness, water flow rates and chamber pressure under the condition of given heating power. Mass transfer coefficients are calculated from the experimental results and then applied in the prediction of water productivity. The maximum discrepancy between the calculation yield and measurement yield is relatively small compared with previous study. In addition, it was found that the yield of the solar still is 23.9% higher when the chamber pressure is lower by 25 kPa due to the enhanced the mass transfer. Similar, doubling the ambient air velocity can increase the water yield by

about 17.0%.

Key words: Vertical tubular solar still; brackish water; mass transfer coefficient; vacuum pressure; mass transfer enhancement

1. Introduction

Fresh and safe water not only is a necessity for healthy human habitation but also for industrial and agricultural production. While water covers approximately 70% of the world, more than 97% of the water is saline and brackish [1], while freshwater is distributed at percentage of 2.53% [2], and only ~0.36% of the fresh water is directly available for human [3]. The demand for fresh water production is growing day by day with the expansion of the population, the development of urbanization and the progress of industrial. Mostly, arid and semi-arid regions are severely affected by facing scarcity of drinking water, water is available, but it is brackish in nature and therefore harmful to human health. Brackish water desalination is believed to be an effective way to solve the shortage of fresh water. However, in current situation nearly 1 kWh of energy is required for desalination process to produce 1.0 m^3 of fresh water [4]. Solar brackish water desalination has become one of more preferred methods for obtaining clear water without CO_2 emission during its life time especially in arid and semi-arid with abundance sunshine. Among solar desalination technologies, Solar Multi Stage Flash (SMSF) and Solar Multi Effect Distillation (SMED) are commercially utilized in cities and always can be made even more economical based on large capacities [5]. However, these technologies are not suitable for remote regions, e.g. the north and the west of China.

Among solar brackish water desalination technologies, solar stills have been considered potentially applicable device to produce clean drinking water to rural, arid and remote communities, which assembles simple, costs effective and operates simple. However, they have the major drawbacks of lower productivity compared with conventional solar desalination methods. The solar still has an efficiency of 30-45% and a less than 5L/m^2/d freshwater yield [6]. By now, many researchers have been involved in their work by structural optimization and redesigning to enhance the productivity and to improve the applicability [7-10].

Kaushal et al. [11] proposed an improved basin type vertical solar still consisting of two closely vertical parallel plates. The evaporation efficiency of the unit was increased compared with previous reported results by other researchers due to better soaking, high rate of temperature equalization within the copper plate. The experimental results show that the cumulative efficiency of the improved still with 10mm partition gap was 10-15% higher than the conventional basin type still. Reddy et al [12] have carried out performance optimization evaluation studies for an active multi-effect vertical solar still using the developed mathematical model. It has been observed that optimum numbers of effects, mass flow rate and gap were found to be five, 7.20kg/h and 0.05m based on the distillate yield and practical conditions.

A novel family scale inflatable plastic solar still was described by Bhardwaj et al [13]. The passive condenser was placed to the basin solar still for providing additional condensation surface. Results indicated that the fresh water yield of the still increased more than 0.95L/h due to the effect of evaporation cooling or an external fan which

suggest that the inflatable plastic still have the potential to provide sufficient drinking water for one family. Estahbanati et al [14] experimentally investigated the effect of the number of stages on the productivity of multi-effect active solar still for the first time. In their work, performances comparison of the continuous and non-continuous model was carried out. Experimental results showed that by increasing the still's number of stages, the positive effect of performances in continuous mode increased outstandingly, which can be predicted by a quadratic function. El-Agouz et al [15] theoretical evaluated the performance for a continuous water flow inclined solar still unit. Three models were studied for the system with and without water close loop. Mostly, the effects of the water mass, water film thickness, water film velocity and air wind velocity on the performance of three models were compared. The results showed that the productivity of the inclined solar still with a makeup water was 57.2% higher than that of a conventional basin-type solar still.

Among the solar stills, the vertical solar stills have been extensively studied using theoretical models and experimental methods, which can be found from the literatures above. However, few investigations on vertical tubular solar brackish water still have been reported. Furthermore, of all the vertical tubular solar stills, it can be clearly seen that the area of the condensing surface of vertical tubular solar still is larger than that of the evaporating surface leading to more yield. However, there is no reported mass transfer correlation for vertical tubular stills, hence, an attempt has been made by this study to determine the mass transfer coefficient of vertical tubular solar still under the conditions of various heating temperature and water flow rates. In additions, this

paper presents an experimental investigation of a single-effect vertical tubular solar brackish water still with a concentric structure, in which the outside of the inner pipe is covered with a wicking layer to provide a uniform of water film. The experimental results will be used to calculate the mass transfer coefficient, based on which the water yield of a vertical tubular solar still can be predicted.

2. Development of single vertical tubular solar brackish water still

2.1. Structure parameters and characteristics

Since the vertical tubular solar brackish water still is believed to be a relatively new way to meet the fresh water demands for remote villages and pastoral areas, e.g. the north and the west of China. However, the optimized operational conditions and mass transfer process were also not fully known. Hence it is necessary to develop a single small scale operational mode and study its performance, before making a full scale device of the present vertical tubular solar brackish water still. The structure diagram of the proposed small scale vertical tubular solar brackish water still mode as shown in Fig.1, and Fig.2 illustrates a schematic and photograph of the experimental set-up.

Fig 1. Structure diagram of vertical tubular solar brackish water still.

Fig 2. Schematic and photograph of the experimental set-up.

The vertical tubular solar brackish water still is compounded of two water collection tanks, a vacuum pump, a heating element, the measurement instruments and two concentric circular stainless steel pipes, which form a gap that are used as distillation chamber, while the innermost pipe also serves as a hot water container.

The outer surface of innermost pipe was covered with water absorption materials (wicking material), which was adhered by wetting the materials and exhausting air between the pipe outer surface and the materials. A horizontal rubber perforated tube which surround across the pipe round, was placed at the top outside bordering edge, on the water absorption materials side of the innermost pipe. The water absorption materials were fed with feed brackish water through several 2 mm diameter holes of perforated tube. An overhead brackish water storage tank with a constant water level was installed for the feed water supply. Brackish water storage tank was connected by a transparent silicone pipe, which entered in the chamber at the bottom of the device and was coiled on the outside surface of the innermost pipe form bottom to top. It is noticed that the feed brackish water is preheated by the hot water container before entering the horizontal rubber perforated tube, which is beneficial to increase the yield. The top edge of water absorption materials was pressed by the rubber perforated tube, and the down edge of that was hung up to just above the perforated tube. In order to overcome the problems of the non-uniform wetting or dry patches along the water absorption materials surface, which lead to poor efficiency of the water absorption materials and hence reducing the distillated yield, several silicone rubber rings were pasted to the water absorption materials at the same interval and cotton thread was stitched into the water absorption materials and form lengthwise horizontal lines and crosswise lines, which means more coarse than conventional wick.

The operational principle of the vertical tubular solar brackish water still is shown in Fig.1. The brackish water from the water storage tank flowed vertically

downwards through the transparent silicone tube into the horizontal rubber perforated tube acting as a water distributor, and then fed the water absorption materials due to gravity. The brackish water in the water absorption materials pasted to the outer surface of the innermost pipe is heated up directly by the hot water inside the pipe, i.e., the hot water container which is powered by the solar collector or the electric heater. As the temperature of container water rises, water vapor formation from the water absorption materials is accelerated and the air in the chamber becomes saturated with vapor. Movement of vapor towards the relatively cold inside surface of the outer pipe occurs due to partial pressure different between the evaporation and the condensation surface. At the same time, the latent heat released by the vapor is lost to the surrounding atmosphere. Desalinated water then naturally flows downwards to the bottom of the device and enters in a freshwater collection tank through the fresh water outlet and the un-evaporated brine leaves the evaporator surface as reject.

Compared with conventional tubular solar still, the several advantages about the designed distillation device can be summarized as follows: (1) The chance of contamination of the freshwater by feed brackish water is nil even for very litter space between the evaporation and condensation surface. (2) Incoming feed brackish water is preheated by the hot water container, which makes the still have more effective evaporation area and freshwater production. (3) The use of the coarse water absorption materials stitched by cotton, several silicone rubber rings and horizontal rubber perforated tube contributed significantly in the uniform wetting area of the still, which is beneficial to the improve of the distillate output. (4) The feed brackish water

enters into the still through gravity feed, which means the vertical tubular solar brackish water still are more easily fabricated and cheaper to use.

2.2. Experimental setup and procedure

The vertical tubular solar still consists of two concentric circular stainless steel pipes (304 grade) having 0.03 m gap between them. The length and diameter of innermost pipe are 0.97 m and 0.10 m respectively. The tubular shell is 0.98 m in length and 0.16 m in diameter. The evaporation area of the operational solar still is 0.295 m^2 and its condensation area is 0.478 m^2.

One thermocouple was fixed in the hot water container to control the operational temperature of the device. Six thermocouples was used to measured the operation temperature and on the outer surface of innermost and outer pipes, respectively. These thermocouples were vertically attached on the outer surface of two pipes at 0.40 m. The evaporation temperature and the condensation temperature of the vertical tubular solar still were reported as an average temperature of the measured points from the three thermocouples on the outer surface. The ambient temperature was measured by another thermocouple placed in the cover. A 20 channel digital recording device was used to record the relevant temperature value. The vacuum pressure inside the device was measured by a piezometer placed on the fresh water collection tank. A valve was used to control the flow rate of the vacuum pump. The feed brackish water flow rate was measured by liquid turbine flow meter and regulated by a needle valve. Instead of solar collector, a U-type electric heating rod was used to provide the power of the device.

All sensors attached on the device and instruments were calibrated before being used to determine their sensitivity. In the experiment, the fresh water yield and the temperature under the operational conditions were recorded at 10 min interval and 1 min interval, respectively. Under the condition of fixed heating temperature, the average yield of four times testing data was adopted as the value of distillate of the device. The instrumentation, their accuracy and range is show below in Table 1.

Table 1 Technical specifications of instruments used in experimental set-up.

3. Determination of mass transfer coefficient of the device

3.1. Heat and mass transfer process in a vertical tubular solar still

The heat and mass transfer process within the vertical tubular solar still is illustrated in Fig.3. The preheated feed brackish water evaporates in the soaked wicking materials and the vapor moves through air towards the condensation surface on the inside of the outer pipe due to the difference in the vapor pressure between the evaporation and condensation surface.

Figure. 3 Heat and mass transfer processes in the device.

In order to simplify analysis, the wet air filled in the device is considered homogeneous. The dry air and water vapor in the mixture can be assumed to be an ideal gas under the atmospheric pressure, respectively:

$$p_a V = m_a R_{ga} T \quad (1)$$

$$p_w V = m_w R_{gw} T \quad (2)$$

The density of the mixture:

$$\rho_m = \frac{m_a + m_w}{V} = \frac{p_a M_a + p_w M_w}{R_o T_{av}} = \rho_a + \rho_w \quad (3)$$

where R_o is the universal gas constant, 8.3145J/(mol·K); R_g is gas constant, $R_g = R / M$; T_{av} is the average temperature between the evaporation surface and condensation surface; p is the average pressure. Subscripts: a is air; w is water vapor.

The vapor in the air on the inner surfaces of the outer pipe is saturated, so the water vapor pressure p_w can be estimated from the inner surface temperature of the outer pipe [16]:

$$p_w = 1000 \times 10^{\wedge}\left(\frac{-2900}{T} - 4.65 \times \log_{10} T + 21.738\right) \quad (4)$$

where T is in K.

3.2 Determination of the mass transfer coefficient in the vertical tubular still

The natural convection heat transfer process within the vertical pipe can be expressed as:

$$Sh = C \times (Gr \times Sc)^n \quad (5)$$

where Sh is Sherwood number, G_r is Grashof number, C and n are empirical correlation constants. Apart from the temperature difference, there is also a concentration difference of the water vapor in the still. Heat transfer from the evaporation surface to the condensation surface is by natural convection, which accelerates mass transfer process of vapor. Especially, because the density of the water vapor is lower than the density of the air, the mass transfer process will also accelerate the heat transfer process. So the Grashof number should be modified, it is given by the equation that be provided by Sharpley et al. [17]:

$$Gr' = \frac{x_l^3 \times \rho^2 \times g}{\mu^2} \times \left(\frac{M_c' T_e}{M_e' T_c} - 1 \right)$$

（6）

where x_l is the characteristic dimension of the convection space, ρ is the density of the mixed gas, μ is the dynamic viscosity, M' is the molar mass of the moist air, T is temperature, the subscripts e is for the evaporating surface, c is for the condensing surface.

M' is given by the following equation:

$$M' = M_a \frac{p_a}{p_T} + M_w \frac{p_w}{p_T} \tag{7}$$

where P_T is the total pressure of the moist air, P_T =101.3kPa. Substituting the Equation (7) into Equation (6) gives:

$$G_r' = \frac{x_l^3 \times \rho^2 \times g}{\mu^2 T_c} \left[(T_e - T_c) + \frac{(p_e - p_c) T_e}{\frac{M_a p_T}{M_a - M_w} - p_e} \right] \tag{8}$$

where M_a is molar mass of the dry air, M_a=28.96 g/mol, M_w is molar mass of the water vapor, M_w=18 g/mol.

The Schmidt number (S_C) in the equation (5) mentioned above is taken by the following equation:

$$S_C = \frac{v}{D_v} = \frac{\mu_m}{D_v \rho_m} \tag{9}$$

where v is the kinematic viscosity of the mixed gas, m^2/s; D_v is the mass diffusion coefficient; μ_m is the dynamic viscosity of the mixed gas, which can be given by the equation from Poling et al. [18] [19]:

$$\mu_m = A_o + A_1 t_{av} + A_2 t_{av}^2 + A_3 t_{av}^3 + A_4 t_{av}^4 \tag{10}$$

$$\rho_m = B_o + B_1 t_{av} + B_2 t_{av}^2 + B_3 t_{av}^3 \tag{11}$$

$$D_v = \frac{0.00143 T_{av}^{1.75}}{p_T M_{aw}^{0.5} \left[\left(\sum_v \right)_a^{1/3} + \left(\sum_v \right)_w^{1/3} \right]^2} \tag{12}$$

where T_{av} is average temperature of the surface evaporation surface and condensation surface, K; $\sum v$ is the molecular diffusion volume of each component in the gas mixture, m^2/s. The coefficients in the above formula are shown in Table 2, M_{aw} is expressed by:

$$M_{aw} = \frac{2}{1/M_a + 1/M_w} \tag{12}$$

Table 2 The value of the coefficient.

The Sherwood number (Sh) in the equation (5) mentioned above is computed by the following equation:

$$Sh = \frac{h_m \times x_l}{D_v} \tag{10}$$

where h_m is the mass transfer coefficient of the device, which can be obtained by the by the following formula:

$$h_m = \frac{m}{A_w (\rho_e - \rho_c)} \tag{11}$$

where m is the water production rate of the device, which can be given in the constant temperature heating experiment; A_w is the area of evaporating surface; ρ_e and ρ_c are the densities of the vapor in evaporation and condensation surface, respectively.

As to the equation (5), C and n for the vertical plate cavity can be obtained in Ref. [20]. But C and n for the closed vertical tubular cavity were seldom reported. So C and n can be obtained based on experiments with vertical tubular chamber for

different surface temperature. Then the mass transfer coefficient of the vertical tubular solar still can be expressed by the following formula [21]:

$$h_m = \frac{h_c}{\rho C_{p,a-w} L_e^{1-n}} \tag{17}$$

$$h_c = \frac{k}{x_l} \times C \times Ra^n \tag{18}$$

where k is working medium thermal conductivity, W/m · K; Ra is Rayleigh number.

4. Results and discussion

A serious of experiments were carried out indoors at an ambient temperature of approximately 26 ^{o}C in Hohhot, China, where the local pressure was approximately 88 kPa, for providing the experimental data to estimate the mass transfer coefficient and improving the yield performance of the device. In the experiment, the different water absorption materials thicknesses were changed adhere to the hot water container, and keep the same electric heater under the condition of fixed power. The experimental process included the heating process, the steady state operational process and the natural cooling process. In this case, freshwater yield and temperatures were measured for the device. The second, the feed brackish water flow rate of the device was adjusted by varying the valve to check the evaporation performance (water flow due to evaporating process) of the water absorption materials. Then, when the operational temperature of the device was controlled, improved yield performance study was done on the tubular vertical solar still at negative pressure.

4.1 Experiments under different water absorption materials thicknesses

Water absorption materials pasted on the hot water container is provided for

allowing preheated feed brackish water to follow as thin film over the evaporating surface. The part wetting of water absorption materials will lead to lower soaking performance of the water absorption materials and hence reducing the estimation accuracy of mass transfer coefficient. From the visual inspection of the water absorption materials which was open to atmosphere after removing the outer pipe, it was found that there was a strong relation between the effective evaporation area and the water absorption materials thicknesses. In this experiment, the water absorption materials of 0.5 mm and of 1.0 mm were selected and compared, respectively. The yield, evaporation temperature and condensing temperature of the device under heating and cooling processes were investigated at the same heating power. In addition, the feed brackish water mass flow rate was 7.2 g/min. The temperature of different measured points of the device was recorded and the 10-minute yield of the device was also recorded. Fig. 4 (a) and (b) show the variation in temperature and distillate output of the device with different water absorption materials thickness, respectively.

Figure. 4 Variation of temperature and distillate productivity of the operational mode with the different water absorption materials thickness.

Fig. 4 (a) and (b) indicate the temperature of measuring points quickly increases at the beginning of the experiment and reaches a relatively maximum value after 6.0 h of operating. Also, the fresh water yield rate of the device will reach a relatively steady state after 6.0 h of heating. At this time, it could be clearly seen that the change of the distillate output is small, the temperature difference between the evaporating

surface and the condensing surface keeps constant. It can also be seen that when the electric heating rod is turned off at 15:20 the variation of the temperature of the water and outer pipe falls sharply. Meanwhile, distillate production continues, the reason is that there has some residual heat in the hot water container, and the temperature of the device has the same variation tend with the yield rate.

For the case shown in Fig. 4 (a), the maximum value of the distillate rate is 237 g/h, the maximum evaporation temperature is 82.57 ^{o}C at 14:50. The maximum value of the yield rate shown in Fig. 4 (b) is 247 g/h, i.e., approximately 10 g more than that shown in Fig. 4 (a). It is noticed that the maximum evaporation temperature shown in Fig. 4 (b) is 82.23 ^{o}C, which is the same as that shown in Fig. 4 (a). The reason behind this phenomenon can be explained as follows: at first, the same power heating of two experimental devices was done in the hot water container, so the maximum evaporation temperature can be obtained at the same operating time. When the water absorption materials of 0.5 mm covered the evaporation sides of the device is replaced by that of 1.0 mm, the coarse and porous level of the evaporation surface are strengthened, which leads to more yield of the device with water absorption materials of 1.0 mm. That is the thick water absorption materials had a better soaking characteristics than the shin one. But too thick water absorption materials have also drawbacks, such as larger thermal resistance, more containing air, et al.

4.2 Experiments under different feed water mass flow rate

To calculate the mass transfer coefficient of the vertical tubular solar still accurately, it is very important that the wetting area of the water absorption materials

maintained to 100%. Apart from the water absorption materials thickness, a relative high temperature film on the evaporation surface is maintained by the feed water mass flow rate will, which is a function of elevation head and fluid frictional resistance [11]. Low feed water mass flow rate caused increased evaporation temperature beyond 90 ^{o}C of the device, which generally leads to the scale formation of the holes of the perforated tube and formation of the decreasing of the effective water absorption materials evaporation area which had an adverse effect on fresh water production. Large feed water mass flow rate caused increased reject brine temperature of the device, which normally leads to the increasing of the heat loss and the decreasing of the GOR (Gain Output Rate) of the device, hence it is always recommended to chose appropriate feed water mass flow rate based on the experimental results.

Two cases at the feed water mass flow rate of 0.12 g/s and 0.19 g/s are experimental investigated under steady heating temperature conditions. For each feed brackish water mass flow rate condition, the operating temperature varies range of 55 ~ 85 ^{o}C, with 5 ^{o}C temperature steps, for the experimental procedure validation. The heating temperature was achieved by an electronic temperature controller. The effect of feed water mass flow rate on the device yield was studied. During the experimental period the hot water container temperature was considered as the operating temperature of the device. The constant water temperature condition must be kept more than 2 hours. The experimental results in the device are obtained in Fig. 5.

Figure. 5 Variation of the yield with heating temperature at different feed water mass flow rates.

Fig. 5 illustrates the effect of the feed brackish water mass flow rate on the device yield under different heating temperature. It can be seen in this figure that the hourly yield of the operational device increases with a decrease of the feed water mass flow rate, increases with increasing of the operating temperature. Distillate yield is found to increase from 248 g/h to 256 g/h at operating temperature of 85 ^{o}C by decreasing the feed water mass flow rate from 0.19 kg/s to 0.12 kg/s. This behavior can be explained by Fig. 6, which shows the temperature difference variation between evaporation surface and condensation surface of the device at different operating temperature. Fig. 6 depicts that the temperature difference at the feed water mass flow rate of 0.12 g/s is larger than that at the feed water mass flow rate of 0.19 g/s, and the temperature difference at two feed water mass flow rates decreases as the heating temperature increased. Moreover, the difference of the two curves at two feed water mass flow rate becomes smaller, along with the increases of operating temperature, which leads to more evaporation.

Figure. 6 The temperature difference between the evaporation and condensation surface of the device with heating temperature.

Actually, decreasing the feed water mass flow rate causes an increase the temperature difference between the evaporation surface and the condensation surface. The raising of the temperature difference of the device naturally leads to a strengthening of the heat transfer driving force between the feed water and the outer pipe, and the raising of the productivity output and the performance of the device.

4.3 Estimation and validation of the mass transfer coefficient

Mass transfer formula proposed by Xie [22], has been used calculate the water production rate of the horizontal tubular solar still. However, there are seldom researchers reported on vertical tubular solar still, which means that there are no C and n values for these devices. In the calculation process, for a falling film along a vertical tube, the value of n is given as o.29 [20]. Taking into account the large number of cases studied, we only present and calculate here the more representative temperature range from 50 ^{o}C to 85 ^{o}C. The calculated results of the C value from the formulas mentioned above and the experimental data are listed in Table 4, for the feed water mass flow rate is 0.12 g/s.

Table 3 The C value in mass transfer coefficient based on the experimental data.

We, thus, determine numerically the C value by calculating average the values of C from experimental data. According to the C and n provided above, the mass transfer coefficient of the vertical tubular solar still is determined, and thus, the distillate production of the device can be predicted. For comparison of the deviation of mass transfer coefficient, our calculated results have been compared with results from previous studies [21]. We present this comparison for a previous single-effect vertical tubular solar still in Fig. 7.

Figure. 7 Comparison of the hourly distillate yield predicted values and experimental values.

From the Fig. 7, freshwater production predicted by the present C value of the empirical correlation was nearly 12.89% lower than the previous prediction. Such that the present empirical correlation predicts values with a 9.86 ~25.04% deviation of

compared with experimental data, which justifies the accuracy and suitability of the present calculation for vertical tubular solar still when the operation temperature varies range of 55 ~ 85 ^{o}C.

Taking into account the experimental and numerical uncertainties quoted before and also the uncertainties of the present studies, there is a good overall agreement, and we thus consider the mass transfer coefficient in the present study as a validation of the freshwater yield prediction.

4.4 Yield improvement of the device under negative pressure

The evaporation rate of solar still can be enhanced to higher levels under negative pressure by vacuum pump, which means that the solar still must have a good bearing pressure characteristic. The vertical tubular solar brackish water still presented in this paper has this advantage. In case of device operation at vacuum pressure, only outer pipe has to bear the external pressure from ambient, the bearing pressure performance of the innermost pipe is significantly negligible.

From the angle of heat transfer process, evacuation of the device helps to decrease the non-condensable air inside the evaporating chamber, which will lead to reduce the resistance for the evaporation heat transfer. Therefore, reduction of operating pressure causes enhanced evaporation of the feed water in the water absorption materials due to its higher heat transfer coefficient which leads to more freshwater yield and little energy consumption [23]. Fig. 8 indicates the average freshwater yields variation at different negative pressure and operation temperature during the experimental period.

Figure. 8 Distillation rate of device in different pressures and heating temperatures.

It can be seen from Fig. 8 that the yield rate tends to increase with the decrease of the vacuum pressure and the increase of the heating temperature of the device. And low vacuum degree has little enhancement on the freshwater productivity. As the decrease of the vacuum pressure progresses, with the rise of heating temperature, the distillate production obviously increases. When the pressure decreases from 100 kPa to 75 kPa at a steady operation temperature of 80 ^{o}C, the water yield rate of the device increases from 209 g/h to 259 g/h, which is nearly 223.75% higher than that of the device at the operating temperature of 50 ^{o}C. This may be explained by Fig. 9, the temperature difference between evaporation and condensation surface decreases as the vacuum pressure decreased and the operation temperature increased. The temperature difference variations in the vertical tubular solar still reveal that reducing the operation pressure of the device accelerates the evaporation and condensation process, leading to a decreased the thermal resistance in the evaporation chamber and inducing a decreased temperature difference.

Figure. 9 The temperature difference between the evaporation and condensation surface of the device in different pressures and heating temperatures.

When the pressure decreases from 100 kPa to 75 kPa at a constant operation temperature of 80 ^{o}C, the temperature difference between the feed brackish water in the water absorption materials and the outer pipe decreased from 6.77 ^{o}C to 4.53 ^{o}C. The same trend with the decreasing vacuum pressure can also be observed for the other cases. The evacuation of the device rejects most of the air from the chamber and

thereby enhances the share of the evaporation heat transfer, which leads to the rapid increase of yield rate.

4.5 Effect of cooling air with evacuation on the production of device

When vertical tubular solar brackish water still operates to satisfy the demand of fresh water under the outdoor conditions, climate condition such as air flow, et al, can affect the solar still productivity. Especially, the distillate yield could be enhanced by providing the external air flow in combination with evacuation. Fig. 10 (a), (b), (c) and (d) shows the effect of the cooling air flow rate on the yield rate of the device at a operating temperature of 50 ^{o}C, 60 ^{o}C, 70 ^{o}C and 80 ^{o}C, respectively. It can be observed from the schematics that the yield at the cooling air flow rate of 2.04 m/s is more than that at the cooling air flow rate of 1.02 m/s by 16.79%, 11.15%, 22.95% and 16.99% respectively at operation pressure of 75 kPa. It reveals that the productivity of the device will increase with increasing the cooling air flow rate, this may be due to the consideration of effect of heat loss from the condensation surface by the air flow.

Figure. 10 Distillation rate of the device in different pressures and cooling air flow rate.

This behavior can also be explained by Fig. 11, which shows that when the cooling air flow rate increases, the condensation temperature of the device at the operating temperature of 80 ^{o}C decreases, that is, the effect of condensation heat transfer is strengthened. As a result, an increased amount of freshwater production can be obtained from the device.

Figure. 11 Variation of the condensation temperature of the device in different pressures and cooling air flow rate.

5. Conclusions

This paper designed a novel single-effect vertical tubular solar brackish water still with preheated feed water tube, which increases the feed water temperature and the effective evaporation area thus can improve the freshwater yield performance. To estimate the mass transfer coefficient of the device accurately, the water absorption materials pasted on the evaporation surface was selected as coarse and porous wick gauze, which was divided into many little evaporation zones by cotton thread, in maintaining a uniform wetting film and hence effective evaporation area of the water absorption materials even with low feed water rates. Apart from this mentioned above, a serious of new designs, such as horizontal rubber perforated tube, silicone rubber ring et al, were accepted to enhance evaporation efficiency.

We conducted experimental investigation with a vertical tubular still indoors to confirm the effect of the water absorption materials thickness and feed water flow rate on the freshwater yield rate performance of the device. Based on the experimental results, the mass transfer process of the device was analyzed, the C value from the empirical correlation was calculated. Experimental were also carried out to study the performance of the vertical tubular solar brackish water still under different evaporating temperature, negative pressure and cooling air with evacuation.

The results from the experimental investigation and theoretical obtained the following conclusions:

1) When the evaporation temperature is approximately 82 ^{o}C, the peak value of the yield rate of the device with water absorption materials of 1.0 cm is more than that of the device with water absorption materials of 0.5 cm by 4.1%, which means that the wetting and soaking performance of water absorption materials of 1.0 cm are appropriate in this device.

2) In the fixed operation temperature experiments, the yield of the device at the feed water mass flow rate of 0.19 g/s can be 248.0 g/h. Under the same heating temperature of 85 ^{o}C, the yield of the device at the feed water mass flow rate of 0.12 g/s increases about 3.23% than that of the device at the feed water mass flow rate of 0.19 g/s.

3) When the water absorption materials is 1.0 cm and the feed water mass flow rate is 0.12 g/s, the C value of empirical correlation is calculated as 1.3, which is capable of predicting values closer to the previous experimental values.

4) This solar still can be operated under vacuum pressure, which can improve the productivity performance. The freshwater yield rate of the device can be 258.7 g/h at P_v=75 kPa and a steady operation temperature of 80 ^{o}C, nearly about more 23.92% than that of the device at normal pressure.

5) When the heating temperature of the device is 80 ^{o}C, the yield at the cooling air flow rate of 2.04 m/s is more than that at the cooling air flow rate of 1.02 m/s by 16.99% at operation pressure of 75 kPa.

Nomenclature

C- constant number

C_p- specific heat, J/(kg·K)

D_v- mass diffusion coefficient, m^2/s

Gr- Grashof number

g- gravitational constant, 9.8 m/s^2

h_m- mass transfer coefficient, m/s

h_c- Convective heat-transfer coefficient, $W/m^2 \cdot K$

Le- Lewis Number

M- molar mass, kg/mol

n- constant number

p_a- dry air pressure, Pa

p_w- vapor pressure, Pa

p_T- total pressure, Pa

Q_{rc}- radiative heat transfer between outer pipe and atmosphere, W

Q_{cc}- convective heat transfer between outer pipe and atmosphere, W

Q_{cw}- convective heat transfer between water surface and humid air, W

Q_{ew}- evaporative heat transfer from water surface to humid air, W

Q_{rw}- radiative heat transfer between water surface and cover, W

R_o- universal gas constant, 8.3145J/(mol·K)

R_g- gas constant, J/(kg·K)

Sc- Schmidt number

Sh- Sherwood number

T_{av}- average temperature, K

t_w - condensation temperature, ^oC.

x_l- feature size, m

v- kinematic viscosity, m^2/s

ρ- density, kg/m^3

μ- dynamic viscosity, $N \cdot s/m^2$

Σ_v- molecular diffusion volume

Subscripts

a- air

e- evaporating surface

c- condensing surface

m- mixed gas

w- water vapor

Acknowledgements

We gratefully acknowledge the financial support for this research provided by the National Natural Science Foundation of China (No. 51666013) Projects.

References

[1] S.W. Sharshir, M.O.A. El-Samadony, G.L. Peng, et al, Performance enhancement of wick solar still using rejected water from humidification-dehumidification unit and film cooling, Appl. Therm. Eng. 108 (2016) 1268-1278.

[2] G. Xiao, X.H. Wang, M.J. Ni, et al, A review on solar stills for brine desalination, Appl. Energy 103 (2013) 642-652.

[3] Z.N. He. Solar thermal utilization, China: Press of University of Science and

Technology of China, 2009. 404.

[4] Matthew D. Stuber, Christopher Sullivan, Spencer A. Kirk, et al, Pilot demonstration of concentrated solar-powered desalination of subsurface agricultural drainage water and other brackish groundwater sources, Desalination 355 (2015) 186-196.

[5] Mohammed Shadi S. Abujazar, S. Fatihah, A.R. Rakmi, et al, The effects of design parameters on productivity performance of a solar still for seawater desalination: A review, Desalination 385 (2016) 178-193.

[6] P. Durkaieswaran, K. Kalidasa Murugavel, Various special design of single basin passive solar still - a review, Renew Sust Energy Rev 49 (2015) 1048–1060.

[7] Mehrzad Feilizadeh, M.R. Karimi Estahbanati, Amimul Ahsan, et al, Effects of water and basin depths in single basin solar stills_ An experimental and theoretical study, Energy Conves. Manage. 122 (2016) 174-181.

[8] S.W. Sharshir, N. Yang, G.L. Peng, et al, Factors affecting solar stills productivity and improvement techniques - A detailed review, Appl. Therm. Eng. 100 (2016) 267-284.

[9] T. Arunkumar, R. Velraj, D.C. Denkenberger, et al. Productivity enhancements of compound parabolic concentrator tubular solar stills, Renewable Energy 88 (2016) 391-400.

[10] H.F. Zheng, Z.H. Chang, Z.L. Chen, et al, Experimental investigation and performance analysis on a group of multi-effect tubular solar desalination devices, Desalination 311 (2013) 62-68.

[11] A.K. Kaushal, M.K. Mittal, D. Gangacharyulu, Development and experimental study of an improved basin type vertical single distillation cell solar still, Desalination 398 (2016) 121-132.

[12] K.S. Reddy, H. Sharon, Active multi-effect vertical solar still: Mathematical modeling, performance investigation and enviro-economic analyses, Desalination 396 (2016) 99-120.

[13] R. Bhardwaj, M.V. ten Kortenaar, R.F. Mudde, Inflatable plastic solar still with passive condenser for single family use, Desalination 398 (2016) 151-156.

[14] M.R. Karimi Estahbanati, Mehrzad Feilizadeh, Khosrow Jafarpur, et al, Experimental investigation of a multi-effect active solar still The effect of the number of stages, Appl. Energy 137 (2015) 46-55.

[15] S.A. El-Agouz, Y.A.F. El-Samadony, A.E. Kabeel, Performance evaluation of a continuous flow inclined solar still desalination system, Energy Conves. Manage. 101 (2015) 606-615.

[16] D. L. Ye, J. H. Hu, Practical Inorganic Thermodynamic Data Handbook, Metallurgical Industry Press, 2002.

[17] Sharpley, Boelter, Evaporation of water into quiescent air from a one –foot diameter surface, Indust. Engng Chem, 30 (1938) 1125-1131.

[18] P. T. Tsilingiris, The influence of binary mixture thermophysical properties in the analysis of heat and mass transfer processes in solar distillation systems, Solar Energy, 81 (2007) 1482-1491.

[19] B.E. Poling, J.M. Prausnitz, J.P.O. Connell, The Properties of Gas and Liquids,

McGraw Hill, New York, 2011 601-633.

[20] A. Baı¨ri, Nusselt-Rayleigh correlations for design of industrial elements: Experimental and numerical investigation of natural convection in tilted square air filled enclosures, Energy Convers. Manage. 49 (2008) 771-782.

[21] Z.H. Chang, Y.J. Zheng, Z.Y. Chen, et al, Performance analysis and experimental comparison of three operational modes of a triple-effect vertical concentric tubular solar desalination device, Desalination 375 (2015) 10-20.

[22] G. Xie, L.C. Sun, Z.Y. Mo, et al, Conceptual design and experimental investigation involving a modular desalination system composed of arrayed tubular solar stills, Appl. Energy 179 (2016) 972-984.

[23] H. Al-Hussaini, I.K. Smith, Enhancing of solar still productivity using vacuum technology, Energy Convers. Manag. 36 (1995) 1047–1051.

Captions of figures

Fig.1 Structure diagram of vertical tubular solar brackish water still.

1-the brackish water inlet; 2-over flow tube; 3-control valve; 4-water film; 5-insulation layer; 6-the horizontal rubber perforated tube; 7-transparent silicone pipe; 8-outer pipe; 9-the water absorption materials; 10-silicone rubber rings; 11-hot water tube; 12-electric heater; 13-water linerboard; 14-piezometer; 15-cold water tube; 16-freshwater tank; 17-valve; 18- brine collection tank.

Fig.2 Schematic and photograph of the experimental set-up.

Fig.3 Heat and mass transfer processes in the device.

Fig.4 Variation of temperature and distillate productivity of the operational mode with the different water absorption materials thickness.

Fig.5 Variation of the yield with heating temperature at different feed water mass flow rates.

Fig.6 The temperature difference between the evaporation and condensation surface of the device with heating temperature.

Fig.7 Comparison of the hourly distillate yield predicted values and experimental values.

Fig.8 Distillation rate of device in different pressures and heating temperatures.

Fig.9 The temperature difference between the evaporation and condensation surface of the device in different pressures and heating temperatures.

Fig.10 Distillation rate of the device in different pressures and cooling air flow rate.

Fig.11 Variation of the condensation temperature of the device in different pressures and cooling air flow rate.

Fig.1

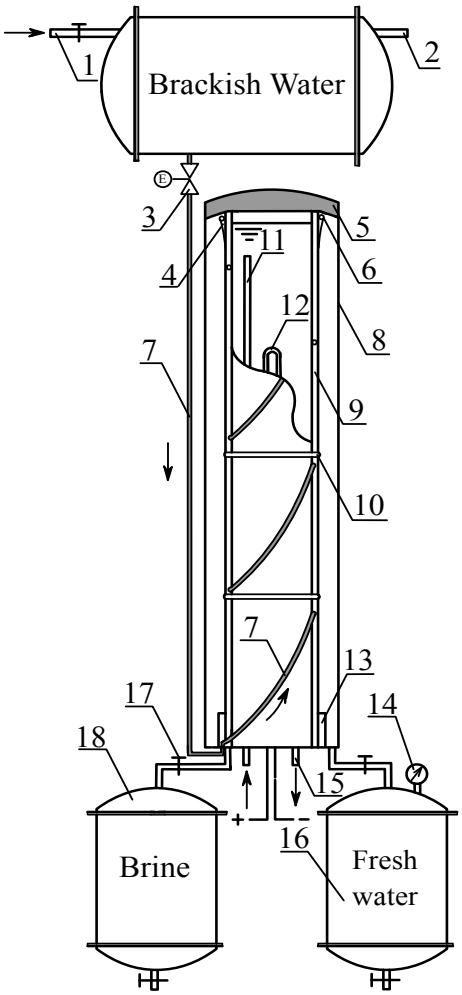
Brackish Water
1
2
3
4
5
6
7
8
9
10
11
12
13
14
15
16
17
18
Brine
Fresh
water
+
–

Fig. 2

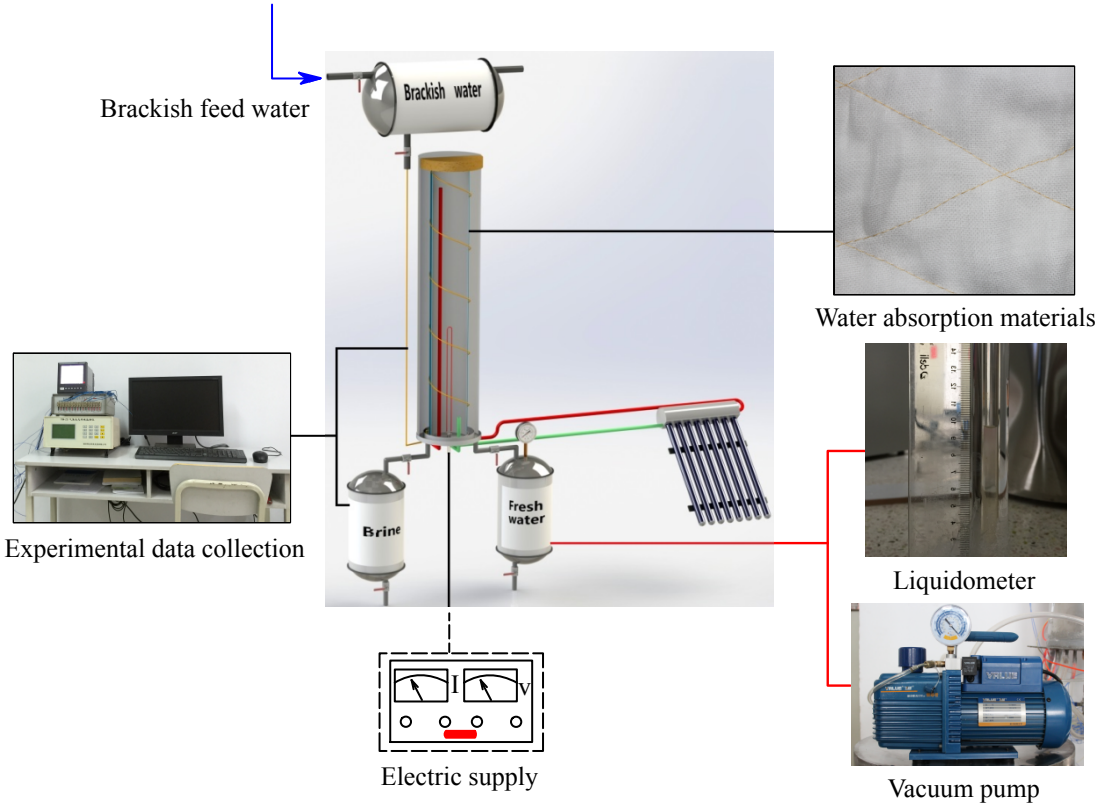
Brackish feed water
Brackish water
Water absorption materials
Experimental data collection
Brine
Fresh water
Liquidometer
I
V
Electric supply
Vacuum pump

Fig. 3

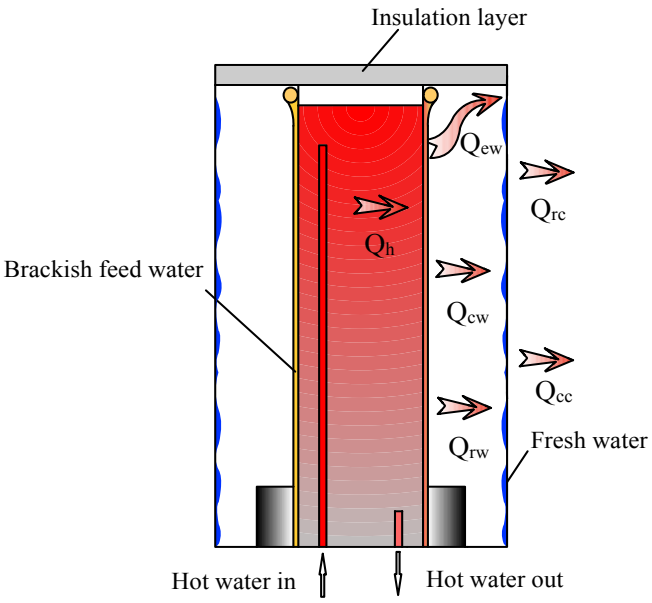
Insulation layer
Qew
Qrc
Qh
Brackish feed water
Qcw
Qcc
Qrw
Fresh water
Hot water in
Hot water out

Fig. 4

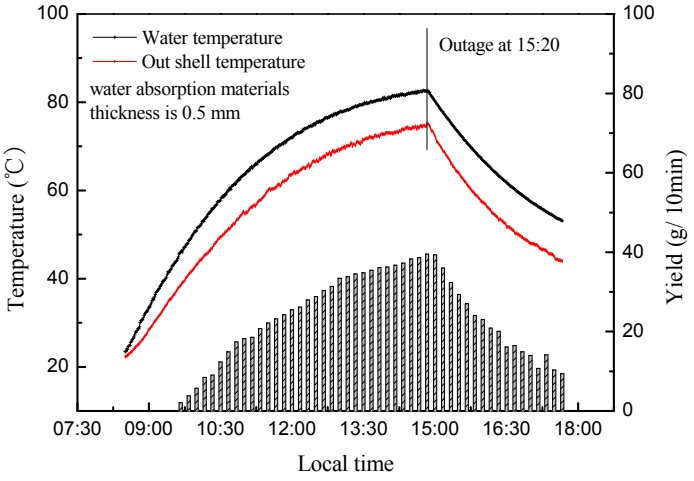
Water temperature
Out shell temperature
water absorption materials
thickness is 0.5 mm
Outage at 15:20
Temperature (℃)
Yield (g/ 10min)
Local time
100
80
60
40
20
0
07:30
09:00
10:30
12:00
13:30
15:00
16:30
18:00

(a)

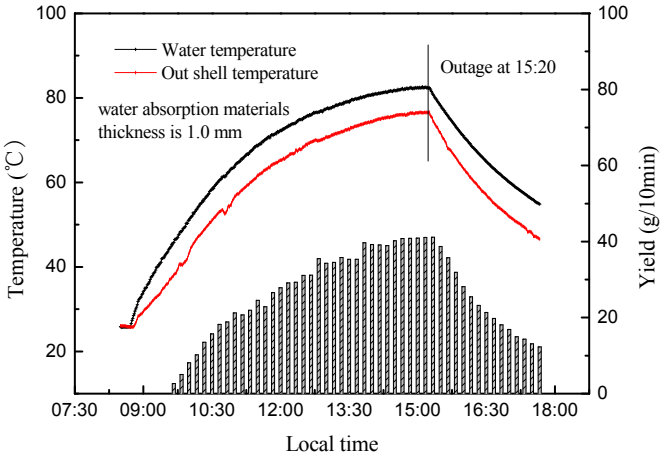
Water temperature
Out shell temperature
water absorption materials
thickness is 1.0 mm
Outage at 15:20
Temperature (℃)
Yield (g/10min)
Local time
100
80
60
40
20
0
07:30
09:00
10:30
12:00
13:30
15:00
16:30
18:00

(b)

Fig. 5

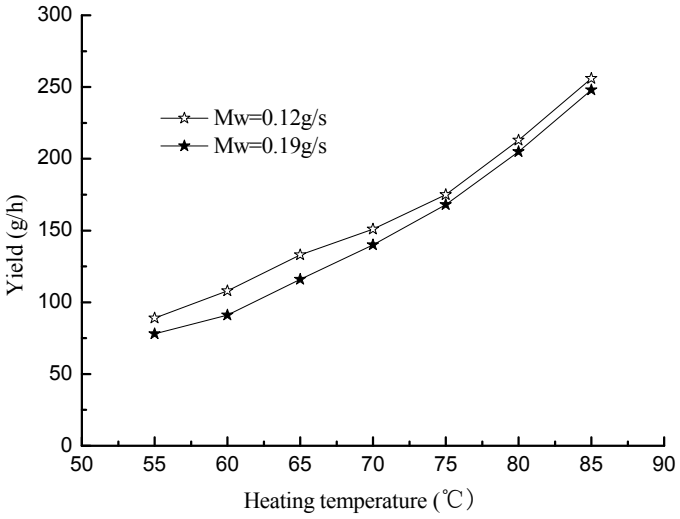
300
250
200
150
100
50
0
Yield (g/h)
Mw=0.12g/s
Mw=0.19g/s
50
55
60
65
70
75
80
85
90
Heating temperature (℃)

Fig. 6

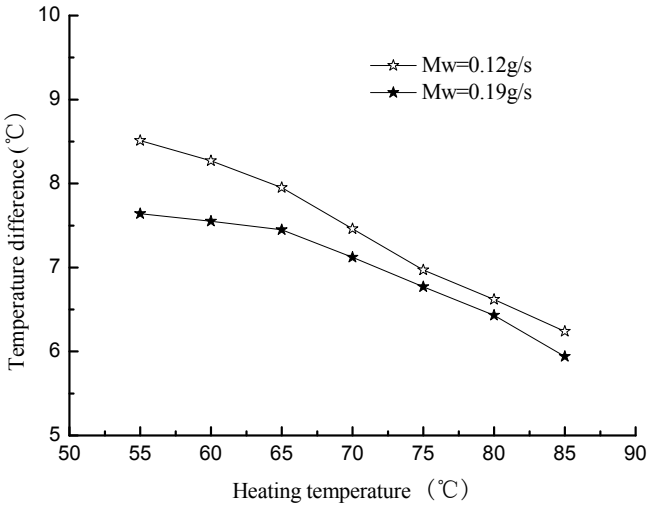
Mw=0.12g/s
Mw=0.19g/s
Temperature difference (℃)
Heating temperature （℃）
10
9
8
7
6
5
50
55
60
65
70
75
80
85
90

Fig. 7

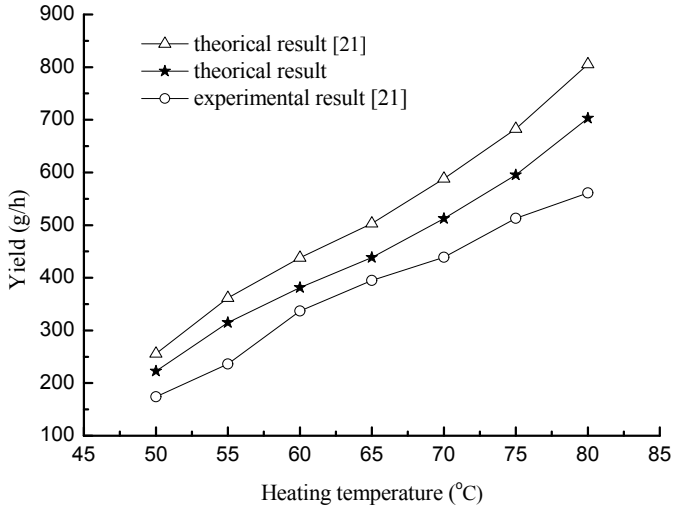
theorical result [21]
theorical result
experimental result [21]
Yield (g/h)
Heating temperature (°C)
900
800
700
600
500
400
300
200
100
45
50
55
60
65
70
75
80
85

Fig. 8

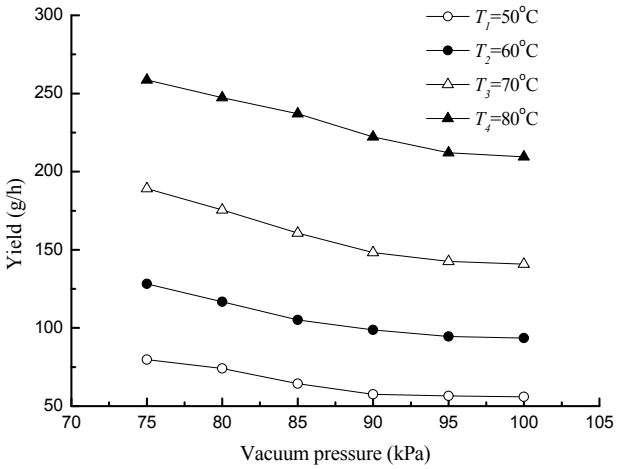
T_1=50°C
T_2=60°C
T_3=70°C
T_4=80°C
Yield (g/h)
300
250
200
150
100
50
70
75
80
85
90
95
100
105
Vacuum pressure (kPa)

Fig. 9

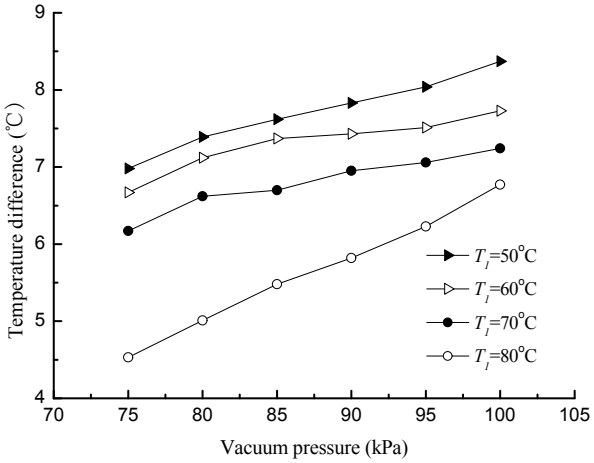
Temperature difference (℃)
Vacuum pressure (kPa)
9
8
7
6
5
4
70
75
80
85
90
95
100
105
T_1=50°C
T_1=60°C
T_1=70°C
T_1=80°C

Fig. 10

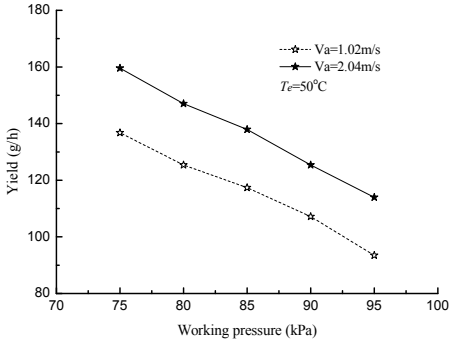
Va=1.02m/s
Va=2.04m/s
Te=50°C
Yield (g/h)
Working pressure (kPa)

(a)

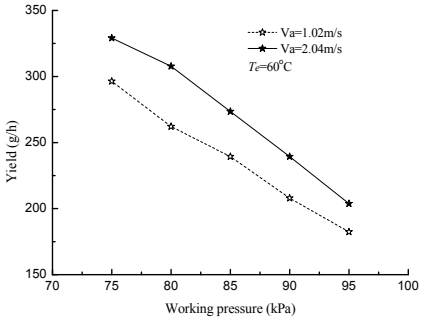
Va=1.02m/s
Va=2.04m/s
Te=60°C
Yield (g/h)
Working pressure (kPa)

(b)

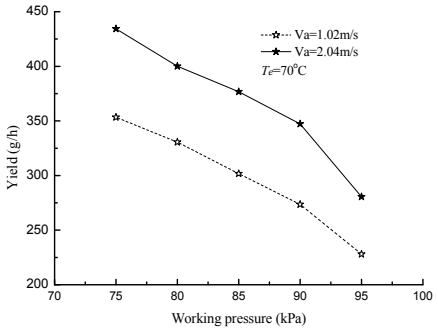
Va=1.02m/s
Va=2.04m/s
Te=70°C
Yield (g/h)
Working pressure (kPa)

(c)

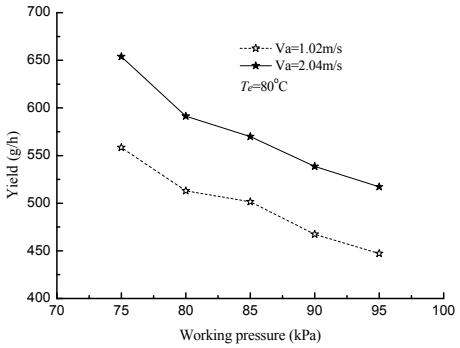
Va=1.02m/s
Va=2.04m/s
Te=80°C
Yield (g/h)
Working pressure (kPa)

(d)

Fig. 11

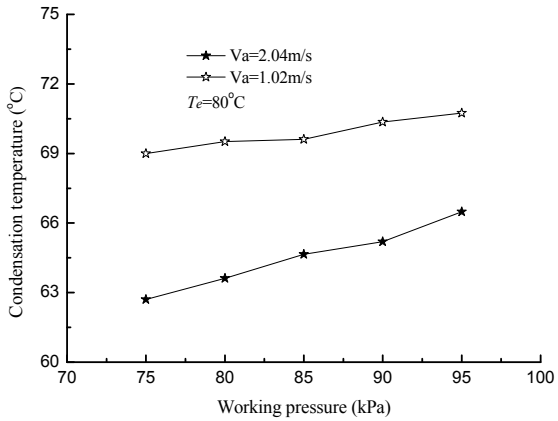
Va=2.04m/s
Va=1.02m/s
Te=80°C
Condensation temperature (°C)
Working pressure (kPa)
75
72
69
66
63
60
70
75
80
85
90
95
100

Captions of tables

Table 1 Technical specifications of instruments used in experimental set-up

Instrumentation	Range	Accuracy
Electronic transformer / TDGC2	0-250 V	± 0.1%
Anemometer / GM8902	0-45 m/s	± 3.0%
Liquid turbine flow meter / Model-109	0.4-4.0 L/h	± 0.1 %
Vacuum pump / V-i180SV	14.4 m^3/h	± 1.0%
Digital weighing balance / HC ES-02	0.01-500 g	± 0.1%
20 channel digital data-recording / TYD-WD	0-300 ^oC	± 0.5 %
Temperature sensor / K	-120-300 ^oC	± 0.5 ^oC

Table 2 The value of the coefficients of Eqs (10) and (11)

（$kg \cdot m^{-3}$）	（$N \cdot s \cdot m^{-2}$）
A_0=1.299995662	$B_0=1.685731754\times10^{-5}$
$A_1=-6.043625845\times10^{-3}$	$B_1=9.151853945\times10^{-8}$
$A_2=4.697926602\times10^{-5}$	$B_2=-2.16276222\times10^{-9}$
$A_3=-5.760867827\times10^{-7}$	$B_3=3.1413922553\times10$
	$B_4=-2.644372665\times10^{-}$

Table 3 The C value in mass transfer coefficient based on the experimental data.

T_e/ °C	T_c/ °C	m/ g/h	Sh	G_r'	Sc	C	∑C/n
50.91	43.93	56.0	2.282	31895.736	0.620	0.130	0.13
56.02	47.51	89.0	2.448	40348.213	0.620	0.130	
60.19	52.46	99.0	2.463	38181.472	0.620	0.133	
61.31	53.92	91.0	2.243	36978.457	0.620	0.122	
65.71	58.25	116.0	2.365	39435.559	0.620	0.126	
70.61	63.29	140.0	2.385	41678.895	0.619	0.125	
75.67	68.89	168.0	2.519	42402.773	0.618	0.132	
79.84	73.07	209.0	2.687	46277.493	0.616	0.137	
80.58	74.15	205.0	2.685	44799.210	0.615	0.138	
85.34	79.10	248.0	2.815	49187.345	0.611	0.142	

Highlights

A novel vertical tubular solar brackish water still is described.

Mass transfer coefficients are calculated from the experimental results.

The maximum discrepancy is relatively small compared with previous study.

The maximum yield can reach 653.89 g/h at operation pressure of 75 kPa.